Roles of water vapor sources and transport in the intraseasonal and interannual variation in the peak monsoon rainfall over East China

Qucheng Chu[1,2] · Qiguang Wang[3] · Guolin Feng[2,3,4] · Zikang Jia[5] · Gang Liu[5]

Abstract

ERA-Interim reanalysis data from 1979 to 2017 are utilized to analyze the intraseasonal and interannual variabilities in the moisture transport associated with the summer rainfall over East China. Three key issues of moisture sources for East China summer precipitation are discussed in this study: the identification of the primary moisture sources of summer precipitation, determination of their individual contributions to the intraseasonal variation in summer precipitation, and determination of the extent to which each source affects the interannual variation in precipitation during the peak monsoon rainfall period (PMRP). Through the Lagrangian method, the water vapor is divided into six sources, namely, the land area source, East China source (EC source, except for the target region), Indian Ocean source (IO source), Pacific Ocean source, South China Sea source, and regional evapotranspiration sources. This study proposes that the rainfall over South China during the PMRP is mainly influenced by the IO source water vapor transport (52.4%). For the middle and lower Yangtze River valley, the rainfall contribution from southwesterly moisture transport accounts for approximately 50% of the total rainfall during the PMRP and determines the intraseasonal and interannual variation in the summer rainfall. The water vapor from terrestrial evaporation, which includes EC source water vapor (38.9%) and North China (NC) source water vapor (21.8%), is the most important moisture source for rainfall over NC during the PMRP.

Keywords East China · Summer precipitation · Moisture source · HYSPLIT

1 Introduction

Climatically, the summer monsoon system over China has a significant effect on water vapor transport, which can have a fundamentally dominant effect on the summer rainfall (Ding and Chan 2005). Hence, the intraseasonal and interannual variations in summer rainfall are determined by the summer monsoon. Previous studies have revealed that water vapor arrives in East China mainly through three branches during the boreal summer (Zhai and Eskridge 1997; Simmonds et al. 1999; Xue et al. 2003; Zhou and Yu 2005; Chan and Zhou 2005; Fan 2006; Fan et al. 2008; Wang and Chen 2012; Li et al. 2013; Chu et al. 2015). The Indian summer monsoon transports water vapor from the Indian Ocean. The water vapor over the Pacific is moved by southeasterly water vapor transport. The water vapor is transported via the western margin of the western Pacific subtropical high. The terrestrial source rainfall originates from Eurasia, which is fundamentally carried by midlatitude westerlies (Dominguez et al. 2006). Moreover, for East China, the effect of regional evapotranspiration on summer monsoon rainfall cannot be ignored. The abovementioned water vapor transport makes the water vapor sources of the summer rainfall over East China more complex than expected (Ma et al. 2004; Pathak et al. 2014).

Based on the station data provided by the China Meteorological Administration (CMA), the rainfall during the boreal summer constitutes approximately 40% of the annual total

✉ Guolin Feng
fenggl@cma.gov.cn

1 State Key Laboratory of Satellite Ocean Environment Dynamics, Second Institute of Oceanography, Hangzhou, China

2 College of Physical Science and Technology, Yangzhou University, Yangzhou, China

3 National Climate Center, China Meteorological Administration, Beijing, China

4 Southern Marine Science and Engineering Guangdong Laboratory, Zhuhai, China

5 College of Atmospheric Sciences, Lanzhou University, Lanzhou, China

rainfall over East China. The anomalous precipitation events can cause severe floods over East China. Hence, the intraseasonal and interannual variation in summer rainfall has been a focus of meteorologists (Ding and Chan 2005; Zhou and Yu 2005; Zhao et al. 2007; Zhu et al. 2011; Sun and Wang 2011, 2015; Li et al. 2013, 2019; Gong et al. 2017, 2019). Ding and Chan (2005) found that water vapor transport from the Sino-Indian Peninsula and South China Sea has a considerable influence on the variation in the summer monsoon rainfall over East China. Zhao et al. (2007) suggested that the southwesterly water vapor transport over East China moves consistently northward during the flood season, as does the associated vertical upward water vapor transport, along with the shift in the main rain band from South China (SC) to North China (NC) via the middle and lower Yangtze River valley (YRV). In addition, Li et al. (2019) found that an anomalous South Asian anticyclone in April is closely associated with an earlier Meiyu onset in June. Moreover, the variations in water vapor transport have a considerable effect on both the interannual variation and intraseasonal variation in the summer monsoon rainfall over East China. Zhou and Yu (2005) proposed that the sources of water vapor associated with the typical anomalous precipitation of China are different from those connected with the mean state during the boreal summer. Li et al. (2013) revealed that the interannual variation in the summer monsoon rainfall over SC is primarily affected by water vapor transport from the Indian Ocean and Bay of Bengal. Although the intraseasonal and interannual variations in the summer rainfall over East China have been widely studied, the corresponding mechanisms have not been clearly illuminated. Thus, to improve the prediction methods for summer rainfall, the water vapor transport processes of summer rainfall should be studied further.

The Eulerian method was extensively used in the abovementioned studies. The Eulerian method can calculate the temporal variations in meteorological elements over a specified region. However, it is difficult to distinguish the contribution from each water vapor source to the summer rainfall based only on the Eulerian method because the water vapor transport processes are not independent of each other (James et al. 2004; Chen et al. 2011; Jiang et al. 2017). For instance, the summer monsoon rainfall influenced by the southwesterly or southeasterly water vapor transport over East China cannot be accurately distinguished by the Eulerian method because the transport processes converge over the South China Sea before arriving in East China. Considering the deficiencies of the Eulerian method, the hybrid single-particle Lagrangian integrated trajectory (HYSPLIT) model (Draxler and Hess 1997, 1998) has been extensively utilized to analyze moisture transport systems (Stohl and James 2004, 2005; Brimelow and Reuter 2005; Perry et al. 2007; Sodemann and Stohl 2009; Van der Ent et al. 2010; Gimeno

et al. 2010; Drumond et al. 2011; Jiang et al. 2013, 2017; Sun and Wang 2014a, b; Pathak et al. 2017). The major advantage of the Lagrangian particle dispersion model is that it can calculate the atmospheric water cycle based on the variation in the water vapor content within the air parcel along its motion trajectory (Sun and Wang 2014a, b).

Based on three-dimensional positioning and meteorological reanalysis data, the HYSPLIT model can calculate the motion trajectory of a specific air parcel. Through the Lagrangian method, Jiang et al. (2013) studied the characteristics of moisture contributions during the boreal summer over the YRV. Chu et al. (2019a) focused on the effect of water vapor transport processes on the variations in the seasonal mean rainfall over East China. Chen and Luo (2018) used the Lagrangian model to explore the paths and sources of the water vapor carried to SC during the preflood season. Moreover, based on a Lagrangian model, Sun and Wang (2014b) quantitatively calculated the water vapor transport from every water vapor source to East China for the 2000–2009 period.

Climatically, the role of the prime moisture source in the variations in summer rainfall over East China is difficult to identify. Many studies have used the Lagrangian method to reconstruct the source-receptor relationship for the mean climate state (Chu et al. 2019a), while few of the studies analyzed the intraseasonal variations in the water vapor transport processes and the relationships with rainfall. Chu et al. (2019b) found that because of the intraseasonal changes in the moisture transport, obvious discrepancies occurred between the interdecadal variabilities in the total rainfall and peak monsoon rainfall over SC during the preflood season. In fact, although the rainfall over SC during the preflood season is mainly influenced by the southwesterly moisture transport, the moisture source is quite different in each month (Chu et al. 2017, 2019b). During the May, the southwesterly water vapor released over SC is carried from the Bay of Bengal. While, during the June, the rainfall over SC is mainly influenced by the southwesterly water vapor transport, which carried the water vapor from the tropical Indian Ocean. It means that the pivotal water vapor source of the peak monsoon rainfall is difficult to be clearly identified through the source-receptor relationship for the mean climate state. It should be noted that the peak monsoon rainfall period (PMRP) is the most important rainfall period over East China during boreal summer. Anomalous persistent torrential rain occurs frequently during the PMRP and causes severe flooding in East China (Zhang et al. 2013). Hence, it is necessary to distinguish the role of each water vapor source in the peak monsoon rainfall.

In this study, the interannual and intraseasonal variations in the moisture transport from each source and their relationships with the peak monsoon rainfall over East China during 1979–2017 are quantitatively calculated by the HYSPLIT

model. The structure of this study is arranged as follows. Section 2 introduces the reanalysis data and Lagrangian method employed in the paper. The intraseasonal variation in the moisture sources and transport in East China are investigated in Sect. 3. The most influential water vapor transport for the interannual variation in precipitation during the PMRPs is discussed in Sect. 4. Finally, Sect. 5 provides the conclusions.

2 Data and methods

2.1 Data

In this paper, the output from the HYSPLIT model is utilized to determine the main moisture sources of East China. Based on the results proposed by Trenberth et al. (2011), the ERA-Interim reanalysis data are the most suitable reanalysis data for capturing water vapor transport. Hence, ERA-Interim 6-hourly reanalysis data are employed as the HYSPLIT model input data in our study. Through these data, the water vapor released in the target region can be backtracked. Then, the water vapor sources of the target region can be found. The output from the HYSPLIT model, which is utilized to describe the trajectories, includes the three-dimensional positions of air parcels (longitude, latitude, and altitude). Moreover, we utilize the ERA-Interim reanalysis data, available at 1° × 1° resolution, to quantitatively calculate the contributions of the water vapor transported from every target source (Emil et al. 2016). The abovementioned calculations utilize a 6-hourly mean evaporation and rainfall dataset from 1979 to 2017.

2.2 Methods

During boreal summer, there are three PMRPs over East China: the preflood season for SC, the Meiyu season for the YRV, and the rainy season for NC (Coching 1934). Essentially, the PMRPs that occur over East China are fundamentally controlled by the East Asian summer monsoon, which gradually moves northward during boreal summer. (Ding et al. 2008; Si et al. 2008). Note that the interannual variations in the summer rainfall over SC, the YRV, and NC are significantly different. Previous studies indicated that strong southeasterly water vapor transport can lead to more summer rainfall over NC and SC and less summer rainfall over the YRV, and vice versa (Zhou and Yu 2005; Ding et al. 2009). The out-of-phase relationship in the summer rainfall over East China is generally led by the western Pacific subtropical high. Hence, the water vapor sources of the summer rainfall over East China should be subdivided. Based on previous studies, Chu et al. (2019a) subdivided East China into three rectangular subregions: SC (105°–120° E, 22°–26° N), the
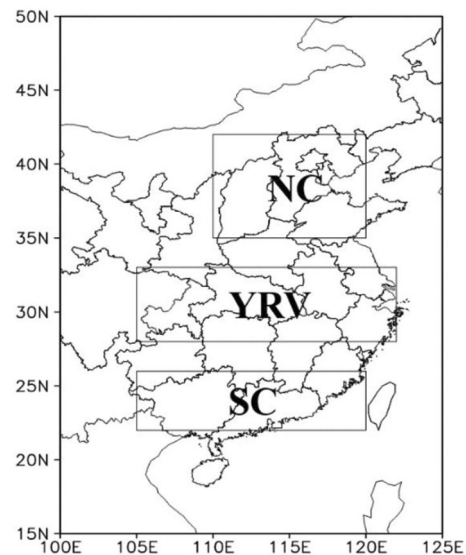
Fig. 1 The three subregions of East China [SC (105°–120° E, 22°–26° N), the YRV (105°–122° E, 28°–33° N), and NC (110°–120° E, 35°–42° N)]

YRV (105°–122° E, 28°–33° N), and NC (110°–120° E, 35°–42° N), as shown in Fig. 1.

A Lagrangian particle dispersion model, namely, HYSPLIT 4.9, which was proposed by Draxler and Hess (1997, 1998), is utilized to calculate the trajectories of a large number of particles representing the air parcels over East China in the period of 1979–2017. Li et al. (2010) indicated that the water vapor is mainly transported below the upper troposphere. Thus, we select to release the particles from the 500 m level to the 3500 m level, with a 500 m interval (seven levels are selected). The particles are released over these regions with a 1° × 1° resolution. Moreover, based on the conclusion of Trenberth et al. (2011), the mean time of one atmospheric water cycle process, which ranges from evaporation to precipitation, is 10 days. Thus, the air parcels over East China are backtracked for 10 days to ensure that the trajectories are of acceptable accuracy. The particles are traced backed every 6 h during the rainy season in SC, the YRV, and NC (1 May to 31 August, 123 days).

The HYSPLIT 4.9 model is utilized to calculate the water vapor sources of the summer monsoon rainfall over East China. For these three subregions of East China, more than 1,000,000 particles representing air parcels are backtracked by the Lagrangian method. To utilize a systematic distribution of the trajectories to concisely introduce the water vapor sources of the summer rainfall over East China, Chu et al. (2019a) used the distribution of air parcels 10 days before reaching the target region to represent the real trajectories.

To reasonably estimate the role of each moisture source in the variation in rainfall in a target region, it is necessary to calculate the variations in the water vapor maintained in

the air parcels along the trajectories. Considering the influences of evapotranspiration and rainfall along the motion trajectories, Sodemann and Stohl (2009) calculated the amount of water vapor transported from the specific evapotranspiration source locations to the target locations. To improve the applicability of the abovementioned method, Sun and Wang (2014a) presented the "areal source-receptor attribution method" to compute the amount of water vapor transported from the examined evapotranspiration sources to a target region. Chu et al. (2019a) revealed that the abovementioned method based on the Lagrangian model is valid and credible and is suitable for studies over East China during the flood season.

The areal source-receptor attribution method proposed by Sun and Wang (2014a, b) mainly includes seven steps for computing the moisture uptake and release along the trajectories from an areal source region to an areal target region. The core of this method is to calculate the moisture uptake and release along the target-bound trajectories of each air parcel. Specifically, the moisture uptake over an examined source region can be obtained by calculating the net moisture gained over the source region. The en route loss can be obtained by proportionally subtracting the moisture released en route from the original moisture uptake region over the examined source region. The contribution to the precipitation in the target domain is thus obtained by calculating the ratio of the moisture released from the examined source region to the total moisture release over the target domain.

3 Roles of water vapor sources in the intraseasonal variation in the summer monsoon rainfall

As shown in Fig. 2, the southwesterly moisture transport trajectories account for 54.6% of the total trajectories arriving in SC, representing the primary branch of moisture transmission in SC (Fig. 2a). Furthermore, 35.4% of the air parcels along the southeasterly moisture transport trajectories arrive in SC. For the YRV, 51.4% of the air parcels originate from the southwesterly moisture transport trajectories, and 31.7% of the air parcels come from the southeasterly moisture transport trajectories (Fig. 2b). In addition, 62.9% of the air parcels that arrive in NC are controlled by midlatitude westerlies. The air parcels coming from the southern region account for 16.8% of the total trajectories arriving in NC (Fig. 2c). However, the trajectories over NC exhibit significant intraseasonal variations. During the NC rainy season (from mid-July to mid-August), which is the main precipitation period, the air parcels come from the southern region, accounting for more than 25% of the total trajectories.
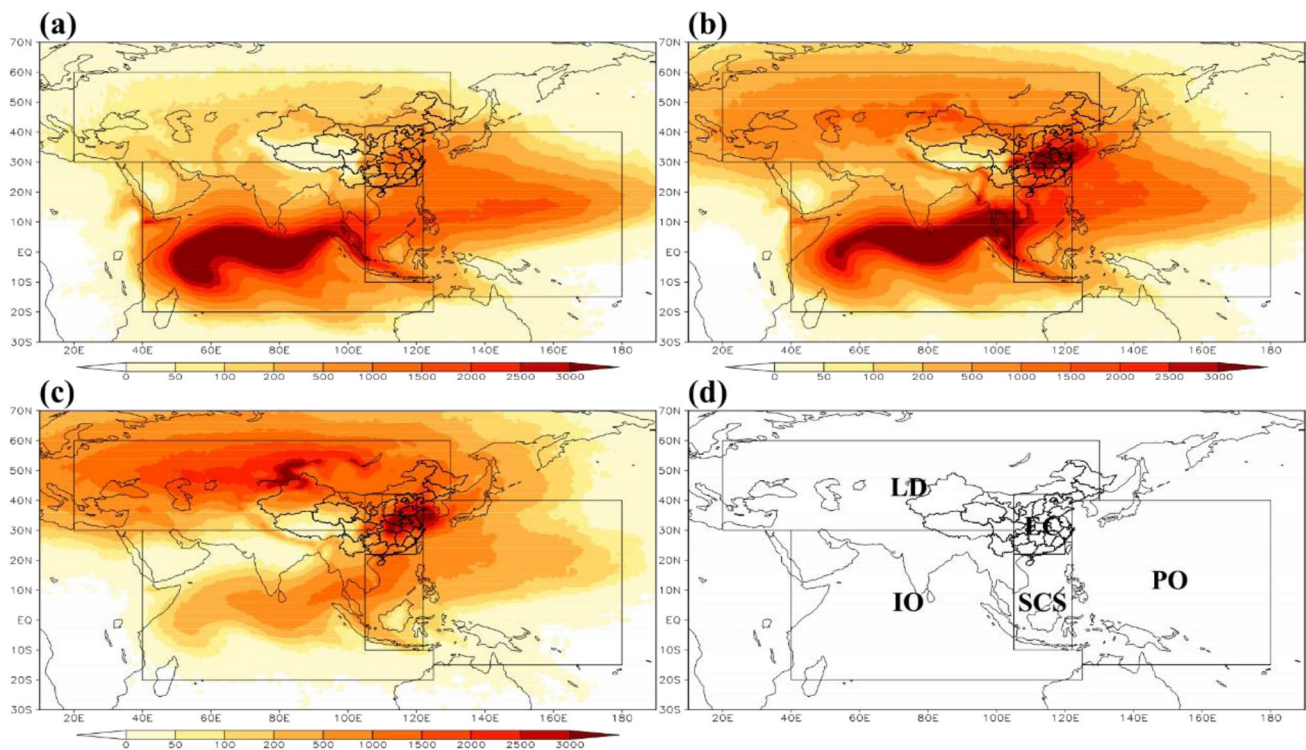

Fig. 2 Spatial distribution of air parcels 10 days before arriving in the **a** SC, **b** the YRV, and **c** NC; **d** regions considered as sources of moisture to the target domain

However, note that a fair number of the air parcels move at higher levels, whereas the evaporation and release of the moisture is mainly cycled at relatively lower levels (Hua et al. 2017). In addition, because the average residence time for moisture in the atmosphere is 10 days, this difference may limit the moisture transport from a given region to a target region. Therefore, the prime source of air parcels may not be the most important moisture source of precipitation over a target region.

Notably, to analyze the effects of water vapor sources on the variations in the peak monsoon rainfall, the local evaporation and precipitation along the air parcel trajectories should be the focus. Notably, the water vapor carried over the South China Sea and East China should be calculated independently because it is influenced by southwesterly and southeasterly moisture transport. Moreover, considering recycled precipitation, the target region should also be considered an independent moisture source (Dominguez

et al. 2006). Accordingly, Chu et al. (2019a) divided the water vapor sources of summer rainfall over East China into six categories. As shown in Fig. 2d, these six moisture sources include the land area source (LD source), East China source (EC source, except for the target region), Indian Ocean source (IO source), Pacific Ocean source (PO source), South China Sea source (SCS source), and target regional evapotranspiration source (SC source, YRV source, and NC source). Then, the mean rainfall contribution originating from every water vapor source that contributes to East China is quantitatively calculated.

For SC and the YRV, the water vapor carried over the IO source and SCS source, which is controlled by the Indian summer monsoon, has the primary effect on the summer rainfall (shown in Fig. 3d, e). The summer rainfall originating from the above-mentioned sources occupies more than 50% of the total summer rainfall over SC (Fig. 4a). Considering the moisture lost en route, a fair
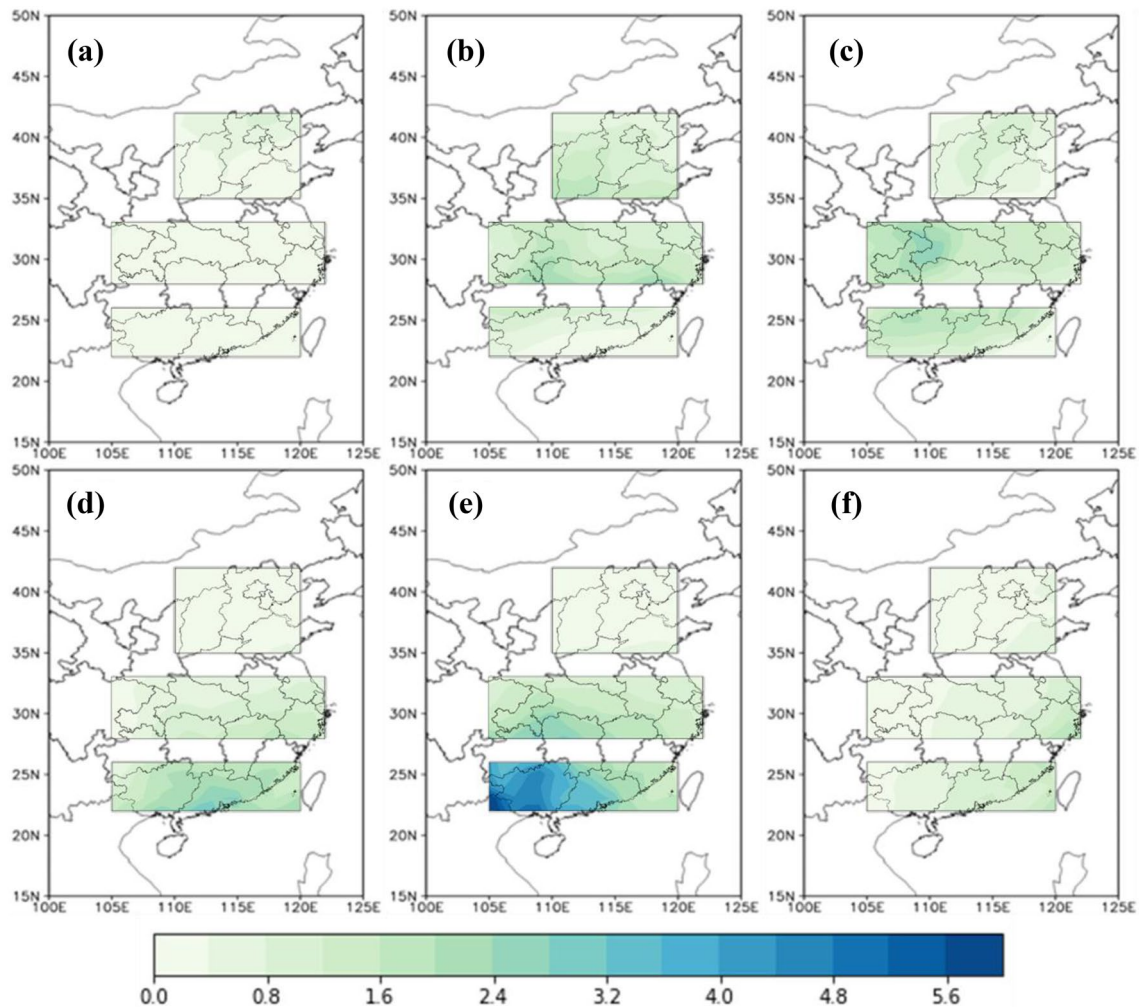

Fig. 3 Moisture contributions from different moisture sources to summer precipitation over East China (mm/day): **a** LD source, **b** EC source, **c** regional evapotranspiration sources (SC source, YRV source, and NC source), **d** SCS source, **e** IO source, and **f** PO source

Fig. 4 Moisture contribution from different land and oceanic sources to daily mean precipitation (mm/day): **a** SC, **b** the YRV, and **c** NC
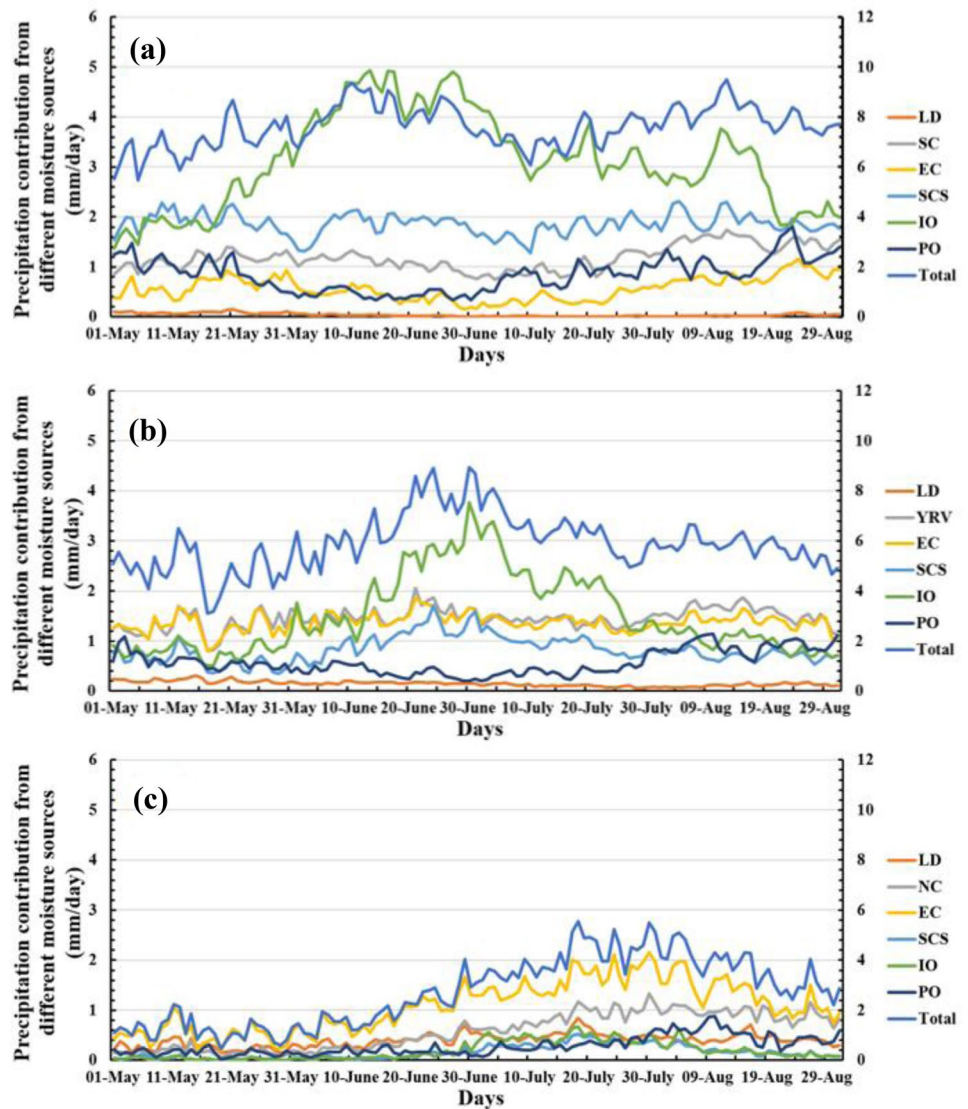
amount of the IO source and SCS source rainfall are lost during the travel of the air parcels. During the boreal summer, there is significant northward water vapor transport over East China. Hence, as shown in Fig. 3b and c, the EC source precipitation and recycled precipitation contribute much less rainfall over SC than over other areas. However, for the YRV and NC, the recycled rainfall accounts for a fair amount of the summer rainfall. The water vapor from the EC source also has a considerable effect on the summer rainfall over the YRV and NC. Moreover, the East-Asia-summer-monsoon-controlled water vapor transport mainly releases water vapor over the southeastern YRV and eastern SC (Fig. 3f). The influence of the LD source moisture transport controlled by the midlatitude westerlies is mainly limited to NC (Fig. 3a). Here, note that significant intraseasonal variations in the primary water vapor transport channel occur over East China during the flood

season. Chu et al. (2019b) found that because of the intraseasonal variabilities in the water vapor transport, there is a significant difference between the interdecadal variabilities of the total rainfall and peak monsoon rainfall over SC during the preflood season. Therefore, the effects of water vapor transport on the intraseasonal variations in summer rainfall are discussed in the following.

The intraseasonal variations in the moisture contribution from each terrestrial and oceanic source to the daily rainfall are shown in Fig. 4. For SC, the YRV, and NC, there are obvious differences in the primary moisture sources of the summer monsoon rainfall. The contribution from the IO source to SC is described by a bell-shaped curve with a maximum contribution during June (Fig. 4a). For the peak IO source contributions, IO source rainfall constitutes more than 50% of the total rainfall over SC. Additionally, the PO source water vapor transport decreases significantly,

led by the enhanced Indian-summer-monsoon-controlled water vapor transport. The water vapor contribution by the SCS source to SC is influenced by both the southwesterly and southeasterly water vapor transport. The southwesterly water vapor transport is the primary moisture source of SC at the onset of the Indian summer monsoon. The southeasterly water vapor transport plays the most important role in the rainfall over SC as the Indian summer monsoon abates. Thus, the curve of the SCS source precipitation over SC is flat during the boreal summer (Fig. 4a). In addition, because the vertically integrated moisture transport over SC is directed southward during the flood season, there is a significant decrease in the moisture carried from terrestrial sources (LD source, EC source, and SC source).

For the YRV rainfall during the PMRP, there are two peaks of summer precipitation. Because of the enhancement in the southwesterly moisture transport, the moisture from the IO source, SCS source, YRV source, and EC source is transported northward. The moisture from the SCS source, YRV source, and EC source rainfall reach and is released over the YRV earlier than IO source moisture, which leads to the first peak (Fig. 4b). Then, there is a significant increase in the IO source rainfall during the second peak. At the same time, the SCS source, YRV source, and EC source rainfall decrease because a fair amount of the moisture from these sources is transported to NC by the enhanced southwesterly moisture transport (Fig. 4b). In addition, Fig. 4b shows that the water vapor carried from the PO source and LD source is reduced during these two peaks. Thus, for the YRV, the Indian-summer-monsoon-controlled moisture transport is the primary moisture transport contributing to rainfall during the PMRP.

The intraseasonal variations in the water vapor transport processes for NC are shown in Fig. 4c. As shown in Fig. 4c, the intraseasonal variations in the summer rainfall are dominated by the water vapor transport processes from the EC source and NC source, which account for more than 50% of the total rainfall over NC. During the PMRP, except at the beginning, the precipitation curve is flat, as observed in Fig. 4c, which means that only a small percentage of the data changes occur because of the water vapor transport from the LD source. In addition, it is observed that the IO source

precipitation over NC decreases during the PMRP, and a further decrease is observed when the contribution from the PO source increases. Note that the peak monsoon rainfall over NC occurs between the end of July and the beginning of August, which is slightly later than the occurrence of the peak of IO source precipitation and slightly earlier than the largest contribution from the PO source. Hence, the major moisture transport channel of precipitation over NC during the PMRP needs to be further discussed.

To illuminate the major water vapor transport during the PMRPs, three time series of a duration of 15 days, the peak of the summer precipitation over SC (P1: 6–20 June), the peak of the summer precipitation over the YRV (P2: 23 June-7 July), and the peak of the summer precipitation over NC (P3: 17–31 July), are selected for further studies. The intraseasonal variations in each water vapor transport process are shown in Table 1. For SC, 4.48 mm/day and 1.96 mm/day water vapor are carried from the IO source and SCS source, respectively, through southwesterly water vapor transport during P1, thus dominating the precipitation during the PMRP (Table 1). Then, during P2, the average values of water vapor carried from the IO source and SCS source to the peak monsoon rainfall over the YRV increased by 1.21 mm/day and 0.29 mm/day, respectively. Furthermore, the variations in the water vapor carried from other sources are minimal (Table 1). For NC, the water vapor transport processes originating from the EC source and NC source have the foremost influence on the intraseasonal variation in the peak monsoon rainfall (Table 1). However, for P3, the water vapor contributions from the IO source and SCS source increased by only 0.17 mm/day and 0.19 mm/day, respectively (Table 1). Compared to those in P2, there is an approximately 50% increase in the rainfall contributions from the IO source and SCS source during P3. During the same period, the moisture contributions from the PO source increase by 0.20 mm/day. This result means that the EC source rainfall over NC is dominated by both the Indian-summer-monsoon-controlled and East-Asian-summer-monsoon-controlled water vapor transport, which carry water vapor from the YRV and SC.

To illuminate the effects of different water vapor sources on the intraseasonal variations in the peak monsoon rainfalls

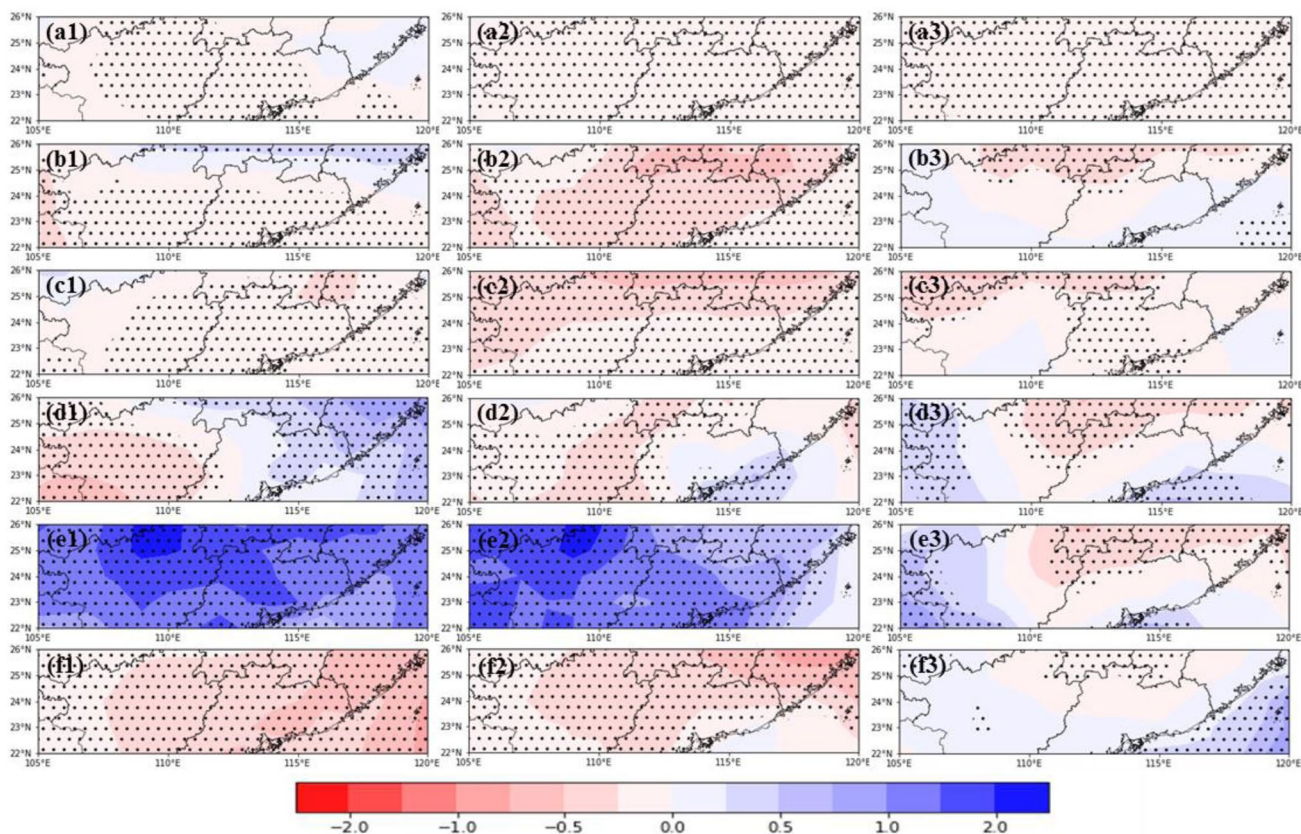| Table 1 Mean moisture contribution from different sources during three intraseasonal time slices	Moisture source (mm/day)	SC			YRV			NC		
		P1	P2	P3	P1	P2	P3	P1	P2	P3
	LD source	0.03	0.02	0.01	0.17	0.15	0.09	0.35	0.49	0.55
	SC/YRV/NC source	1.15	0.89	1.13	1.48	1.56	1.36	0.29	0.57	1.03
	EC source	0.47	0.27	0.43	1.45	1.51	1.29	0.77	1.26	1.83
	SCS source	1.96	1.76	1.87	0.98	1.27	0.84	0.05	0.21	0.40
	IO source	4.48	4.21	3.17	1.78	2.99	1.79	0.05	0.29	0.46
	PO source	0.46	0.27	0.43	0.42	0.31	0.48	0.18	0.18	0.38

Fig. 5 Mean moisture contribution from six moisture sources (top)–(bottom): LD source, EC source, SC source, SCS source, IO source, and PO source to the precipitation over SC during three time slices [(left) P1–(right) P3] (mm/day, dark spotted areas show significance at the 0.1 level)

over East China, we analyze the spatial variations in the water vapor carried from the abovementioned water vapor sources and released over the target regions (shown in Figs. 5, 6, 7). Moreover, the PMRPs denote the foremost consistent rainfall period over East China, which is connected with strongly converged water vapor transport. The daily mean anomalies in the vertically integrated moisture transport and vertically integrated moisture flux divergence during the PMRPs based on composite analysis are shown in Fig. 8, and an anomalous anticyclone shift northwestward over the western North Pacific can be observed during the boreal summer (Fig. 8).

During P1, because of the enhancement in the Indian-summer-monsoon-controlled water vapor transport, there is a positive anomaly of westerly water vapor transport over SC (Fig. 8a). For SC, the rainfall increases a fair amount, led by the increase in the IO source water vapor transport (Fig. 5e1). Meanwhile, the meridional water vapor transport from the SCS source increases significantly, being primarily affected by the western Pacific subtropical high (Fig. 8a). There is an obvious increase in the peak monsoon rainfall over eastern SC, and the main increase in the water vapor originates from the SCS source (Fig. 5d1). Furthermore, for

the southeastern YRV, the significant increase in rainfall is primarily influenced by the Indian-summer-monsoon-controlled water vapor transport, which carries water vapor from the IO source, SCS source, and SC source (Fig. 6c1, d1, and e1). During this period, the oceanic source moisture transport has minimal influence on the precipitation over NC.

During P2, a significant enhancement in the meridional water vapor transport over southeastern China occurs, induced by the shift in the western Pacific subtropical high (Fig. 8b). Meanwhile, there is a negative anomaly of water vapor flux divergence over the YRV region. Because of the anomalous anticyclone, it is difficult for the water vapor carried from the PO source to be directly transported to East China. Therefore, during the PMRP, a significant reduction occurs in the PO source water vapor transport to East China (Figs. 5f2, 6f2). Both the Indian-summer-monsoon-controlled and East-Asian-summer-monsoon-controlled water vapor is transported via the South China Sea before arriving in East China. Hence, during PMRPs, the meridional water vapor motion from the SCS source enhances significantly. The Indian-summer-monsoon-controlled water vapor transport has the foremost effect on the peak monsoon rainfall over the YRV, which leads to a significant
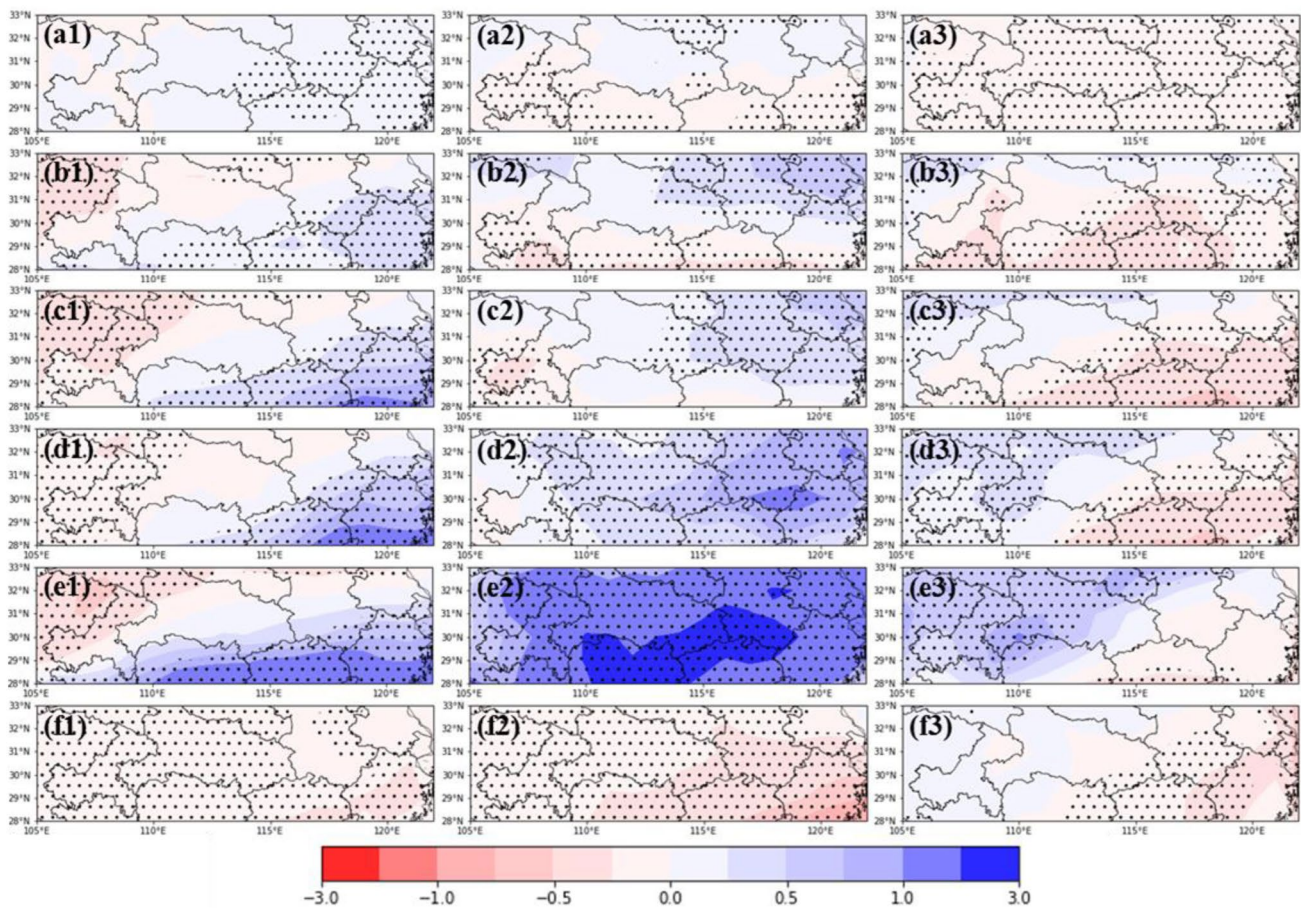
Fig. 6 Mean moisture contribution from six moisture sources (top)–(bottom): LD source, EC source, SC source, SCS source, IO source, and PO source to the precipitation over the YRV during three time slices [(left) P1–(right) P3] (mm/day, dark spotted areas show significance at the 0.1 level)

increase in the rainfall over the whole YRV (Fig. 6e2). Furthermore, the increase in the rainfall over the eastern YRV is mainly affected by the SCS source and SC source water vapor transport (Fig. 6c2, d2). Therefore, the increase in SC source water vapor transport is primarily influenced by oceanic water vapor transport, which carries water vapor from southern China. In addition, during P2, the peak monsoon rainfall over NC is primarily controlled by terrestrial source moisture transport. The increase in the LD source, SC source, and EC source water vapor transport leads to a significant increase in the rainfall over northeastern NC (Fig. 7a2, b2, c2).

During P3, because of the shift in the western Pacific subtropical high, the northwest Pacific anticyclone moves northwestward. The westerly moisture transport anomalies, via the southern bound of the northwest Pacific anticyclone, decrease the zonal moisture transport over southeastern China. There is a negative anomaly of water vapor flux divergence over NC (Fig. 8c). Meanwhile, a

significant anomaly of southerly moisture transport over NC is observed. Therefore, the water vapor contribution from oceanic water vapor transport sources to the rainfall over NC increase significantly (Fig. 7d3, e3, f3). However, the water vapor carried from terrestrial sources, including the EC source and SC source, has important effects on the peak monsoon rainfall over NC during P3 (Fig. 7b3, c3). Note that the anomalous center of the westerlies-controlled rainfall is over northern NC (Fig. 7a3). The anomalous center of the SC source rainfall is over southern NC (Fig. 7c3). The abovementioned results mean that a fair amount of the land evapotranspiration water vapor released over NC is primarily controlled by southwesterly and southeasterly water vapor transport, which carries the water vapor from southeastern China.

In summary, the intraseasonal variations in the peak monsoon rainfall over the YRV and SC are principally affected by the Indian-summer-monsoon-controlled water vapor transport. The intraseasonal variation in the peak monsoon rainfall over NC is influenced by both the
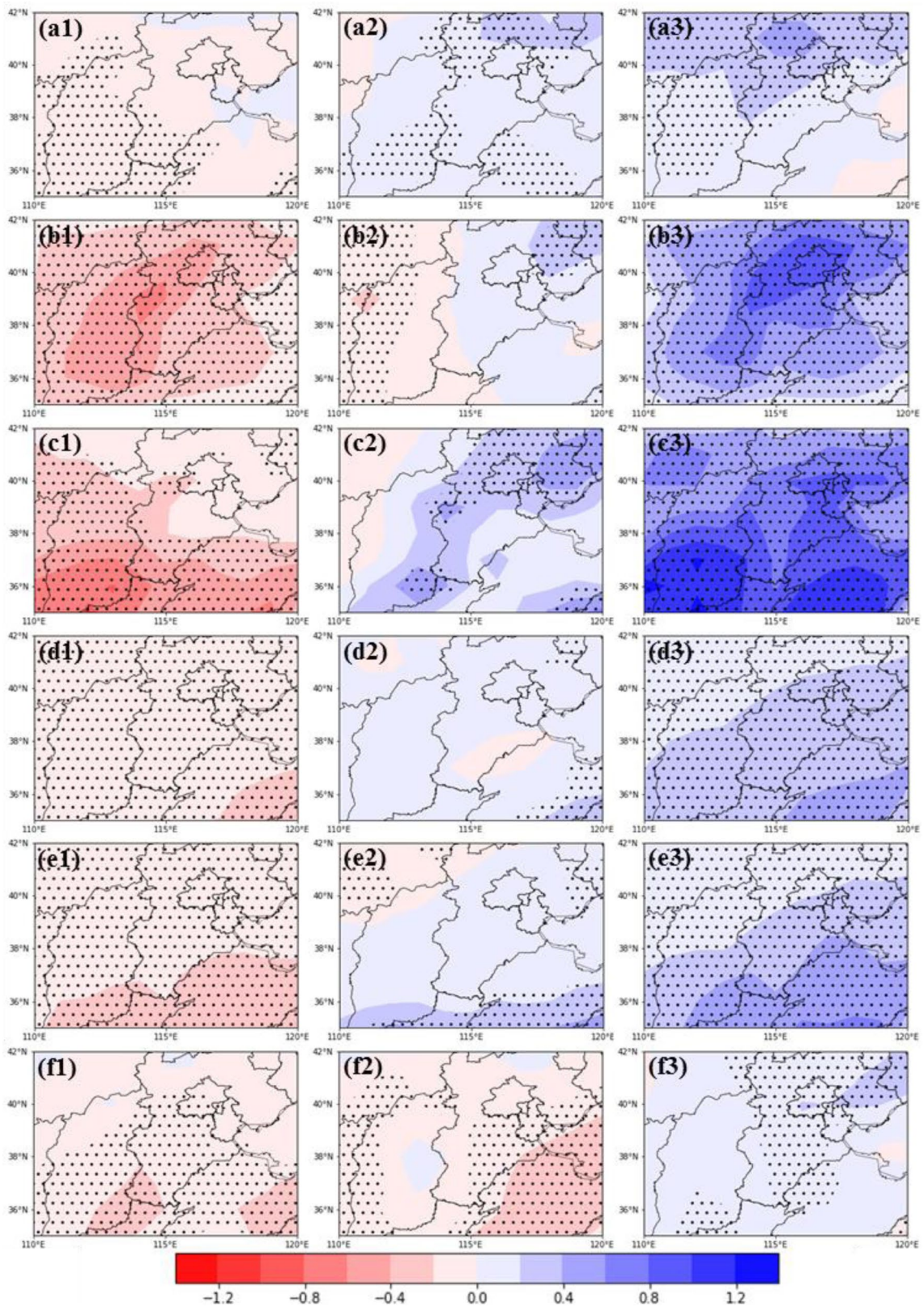
Fig. 7 Mean moisture contribution from six moisture sources (top)–(bottom): LD source, EC source, SC source, SCS source, IO source, and PO source to the precipitation over NC during three time slices [(left) P1–(right) P3] (mm/day, dark spotted areas show significance at the 0.1 level)
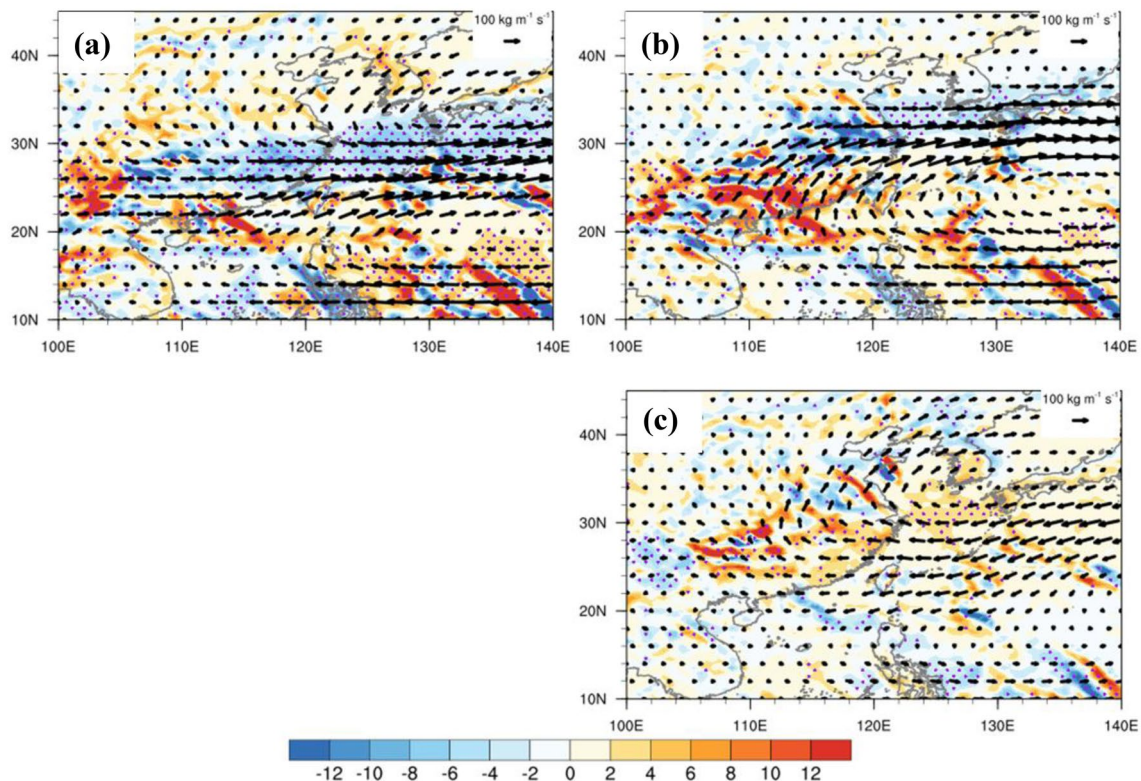
Fig. 8 Mean anomalies of vertically integrated water vapor transport (vector, 100 kg/m/s) and vertically integrated water vapor flux divergence (shading, mm/day) during **a** P1, **b** P2, and **c** P3 (purple spotted areas show significance at the 0.1 level)

Indian-summer-monsoon-controlled and East-Asian-summer-monsoon-controlled water vapor transport processes, which carry water vapor from southeastern China.

4 Roles of the water vapor sources in the interannual variation in the peak monsoon rainfall

The persistent rainfalls over East China during PMRPs determine the effect on the spatiotemporal characteristics of the total rainfall during the boreal summer (Chu et al. 2019b). Anomalous persistent torrential rain can often cause severe floods (Shen et al. 2007; Chu et al. 2016). Considering the differences in the water vapor transport channels over East China, the related mechanisms controlling the climate dynamics of these moisture transport channels are complex and different. Simplifying the moisture transport system over East China benefits the forecasting of the summer rainfall and even the shift in the summer rain belt. Based on the conclusions in Sect. 3, the peak monsoon rainfall is induced by moisture transport from individual moisture sources (Fig. 4). Hence, it is necessary to study the influence of the primary water vapor sources and channels during the PMRPs.

Climatically, the IO source rainfall determines the amount of monsoon rainfall over the YRV and SC during the PMRPs (Fig. 4). The rainfall over NC is significantly affected by the EC source moisture transport. However, the interannual variations in the PMRPs should be considered in the study of the primary moisture source in the peak monsoon rainfall. Hence, based on a 15-day running mean method, the PMRPs, which have the most precipitation during the rainy season, are picked out from the preflood season, mei-yu season, and rainy season period provided by CMA for each year. Then, to illustrate the role of the primary moisture source in the interannual variation of peak monsoon rainfall, the linear trends of the daily mean rainfall and moisture contribution from the primary moisture source were removed before the aforementioned linear regression. The time series of the daily mean rainfall and moisture contribution from the primary moisture source during PMRPs are shown in Fig. 9. The correlation coefficients for the detrended time series of the daily mean rainfall and moisture contribution from the primary moisture source are significant at the 99% confidence level. Based on Figs. 9 and 10 years that exhibit the strongest (weakest) rainfall during PMRPs are selected as the strong (weak) rainfall years. For PMRPs in the strong and weak rainfall years, the amount of water vapor carried from every water vapor source to the target regions is
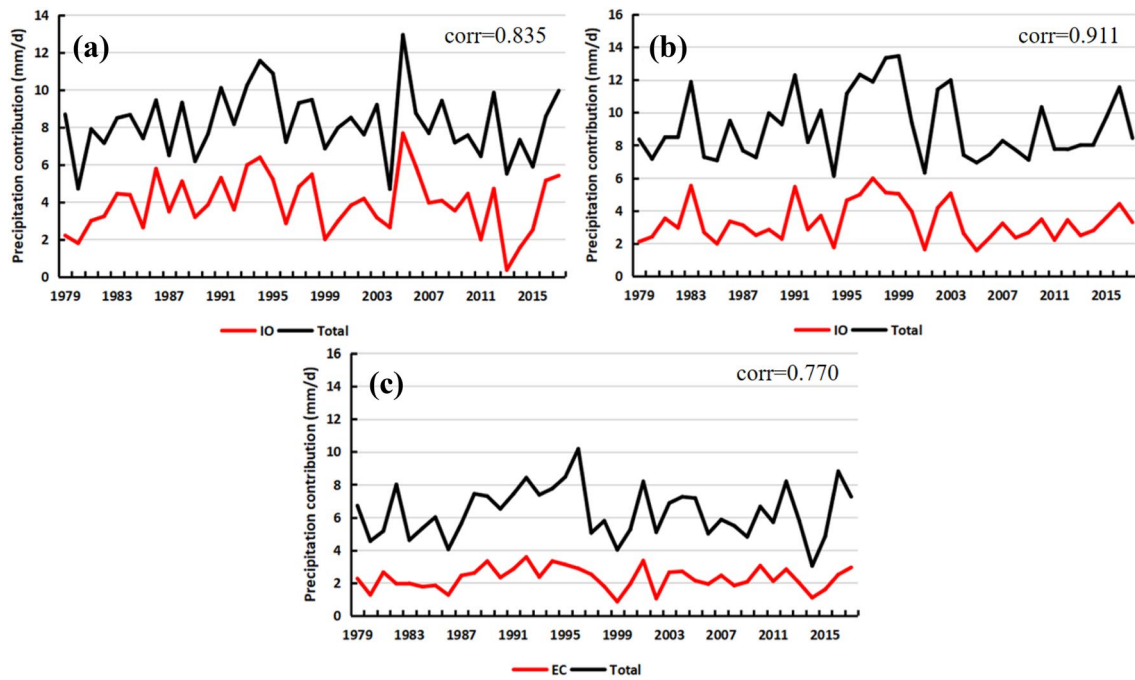
Fig. 9 Time series of daily mean precipitation and moisture contribution from the major moisture source (mm/day): **a** SC, **b** the YRV, and **c** NC
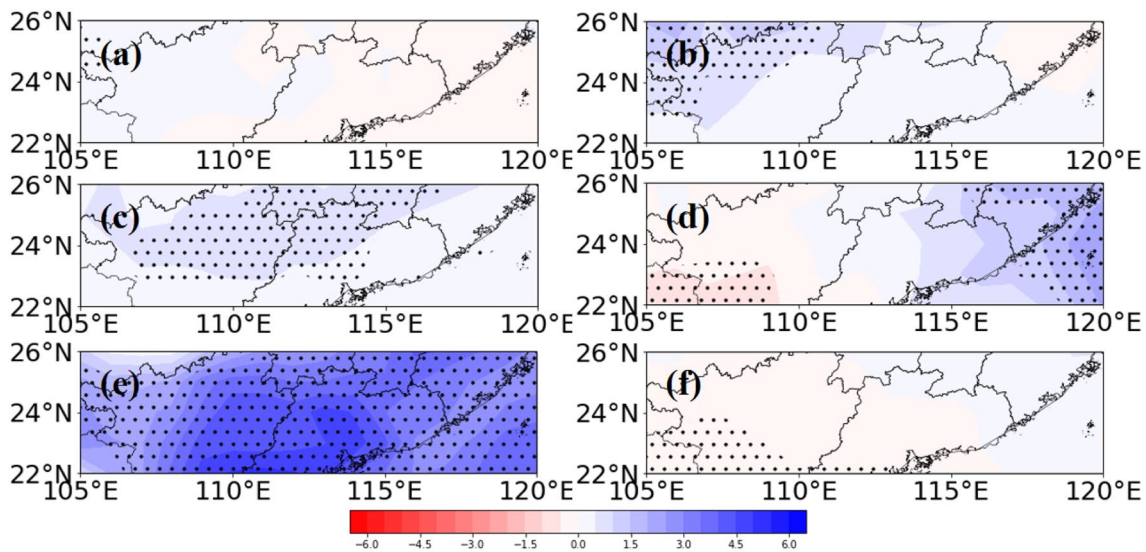

Fig. 10 Differences (strong–weak) in moisture contributions from six moisture sources: **a** LD source, **b** EC source, **c** SC source, **d** SCS source, **e** IO source, and **f** PO source to the precipitation over SC during the PMRP (mm/day, dark spotted areas show significance at the 0.1 level)

calculated (Table 2). For SC, the difference in the IO source rainfall between the strong and weak rainfall years is 3.19 mm/day (Table 2). For the strong rainfall years, the average rainfall contribution from the IO source to the YRV region increases by 2.84 mm/day (Table 2). As Table 2 shows, for strong rainfall years, the average water vapor transport from the EC source to the NC region increases by 1.33 mm/day. Furthermore, note that the LD source rainfall, which is

controlled by the moisture transport due to the midlatitude westerlies, increases only by approximately 0.2 mm/day.

The differences in the water vapor transport processes from six water vapor sources to the rainfall over East China during PMRPs are shown in Figs. 10, 11, and 12. For the peak monsoon rainfall over SC, an obvious increase in rainfall occurs over SC because SC receives a fair amount of atmospheric water vapor from the IO source (Fig. 10e). For

Table 2 Mean moisture contribution from different sources during strong and weak precipitation years

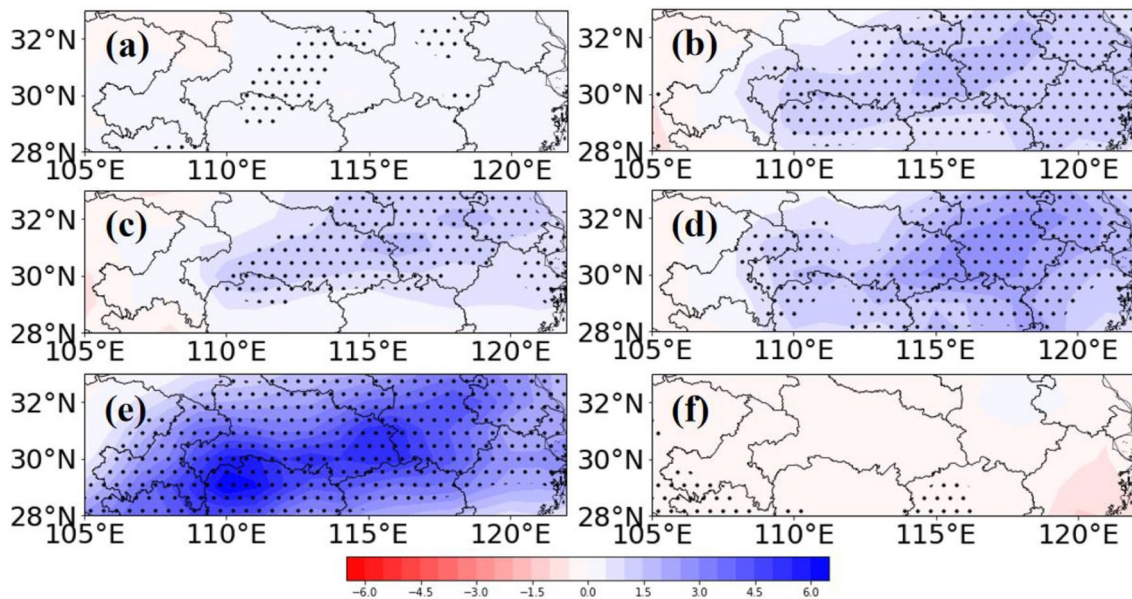| Moisture source (mm/day)	SC		YRV		NC	
	Strong	Weak	Strong	Weak	Strong	Weak
LD source	0.03	0.03	0.22	0.14	0.81	0.59
SC/YRV/NC source	1.45	1.07	2.11	1.60	1.72	1.00
EC source	0.66	0.32	2.22	1.48	2.96	1.63
SCS source	2.47	2.01	2.30	1.12	0.62	0.28
IO source	7.16	3.97	5.18	2.34	0.76	0.37
PO source	0.45	0.47	0.24	0.44	1.13	0.38

Fig. 11 Differences (strong–weak) in moisture contributions from six moisture sources: **a** LD source, **b** EC source, **c** YRV source, **d** SCS source, **e** IO source, and **f** PO source to the precipitation over YRV during the PMRP (mm/day, dark spotted areas show significance at the 0.1 level)

the strong rainfall years, the distribution of the peak monsoon rainfall over the YRV is determined by the IO source water vapor transport (Fig. 11e). During the same period, the PO source and LD source rainfall, which are controlled by the moisture transport from the southeast and midlatitude westerlies, respectively, only slightly change (Fig. 11a, f). Therefore, the increase in the EC source, YRV source, and SCS source water vapor transport is mainly influenced by the southwesterly moisture transport (Fig. 11b, c, d). As shown in Fig. 12c, for the peak monsoon rainfall over NC, the interannual variation is foremost affected by the EC source water vapor transport. The anomalous EC source moisture, which originates from the YRV and SC, is mainly released over western NC. Furthermore, a significant increase occurs in the IO source, SCS source, and PO source water vapor transport (Fig. 12d, e, f). This means that the interannual variation in the peak monsoon rainfall over NC is affected by southwesterly and southeasterly water vapor transport.

The results above suggest that the rainfall contribution from the primary moisture source dominates the spatiotemporal characteristics of the rainfall during PMRPs. Hence, the precipitation contribution from the primary moisture source can be used instead of the total precipitation, which is beneficial for simplifying the related mechanisms controlling the climate dynamics of summer precipitation over East China. As shown in Figs. 13 and 14, the detrended time series of the peak monsoon rainfall over SC, the YRV, and NC is used to regress the anomalies of evaporation and vertically integrated water vapor transport.

A previous study indicated that East-Asian-summer-monsoon-controlled water vapor transport mainly manifests as meridional water vapor transport, while Indian-summer-monsoon-controlled water vapor transport mainly manifests as zonal water vapor transport during the boreal summer (Huang et al. 1998; Zhang 2001) found that strong meridional water vapor transport always corresponds to weak zonal water vapor transport over southern China. The

Fig. 12 Differences (strong–weak) in moisture contributions from six moisture sources: **a** LD source, **b** EC source, **c** NC source, **d** SCS source, **e** IO source, and **f** PO source to the precipitation over NC during the PMRP (mm/day, dark spotted areas show significance at the 0.1 level)
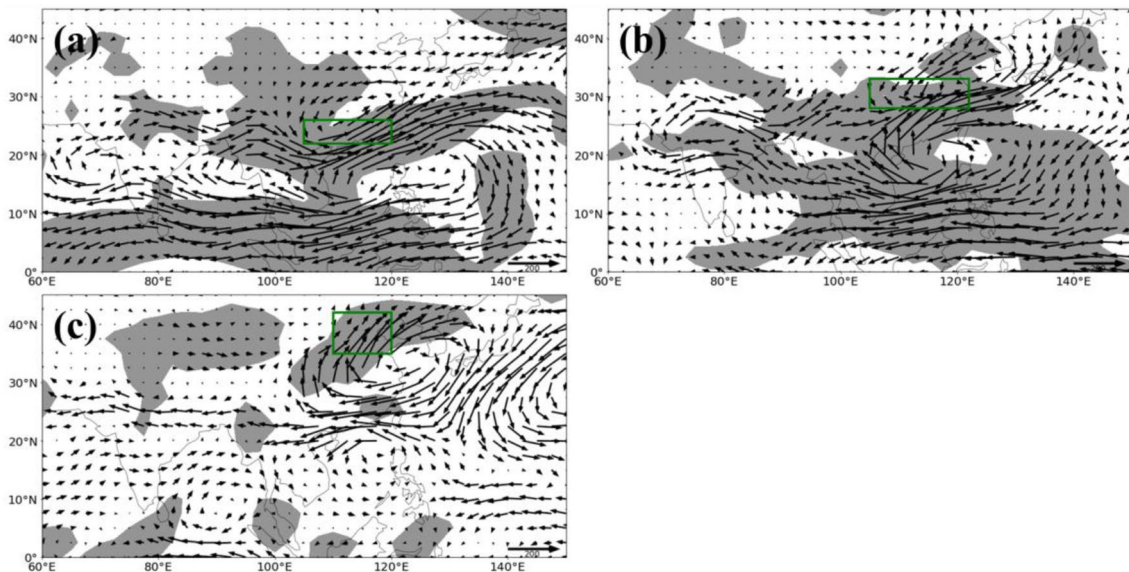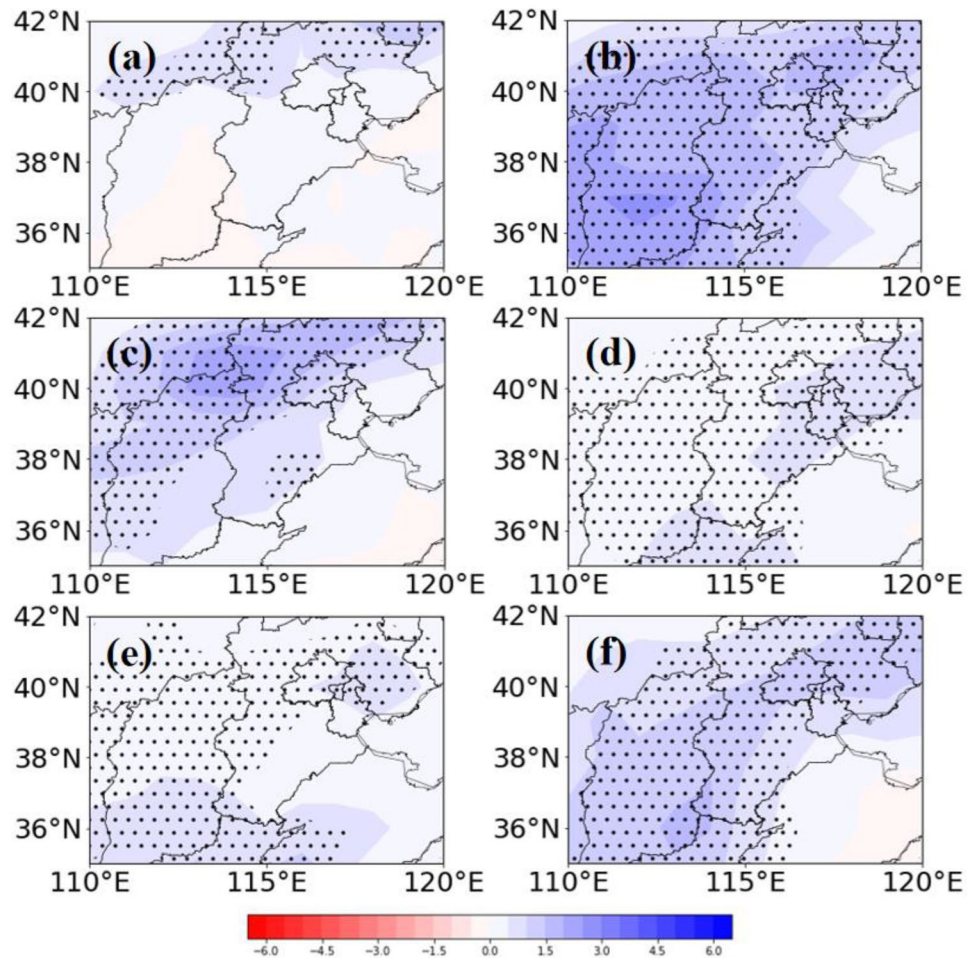

Fig. 13 Anomalies of vertically integrated water vapor transport (vector, kg/m/s) regressed on the detrend time series of **a** the IO source precipitation over SC, **b** the IO source precipitation over the YRV, and **c** the EC source precipitation over NC during PMRP (light-gray shadings denote significance at the 0.1 level)
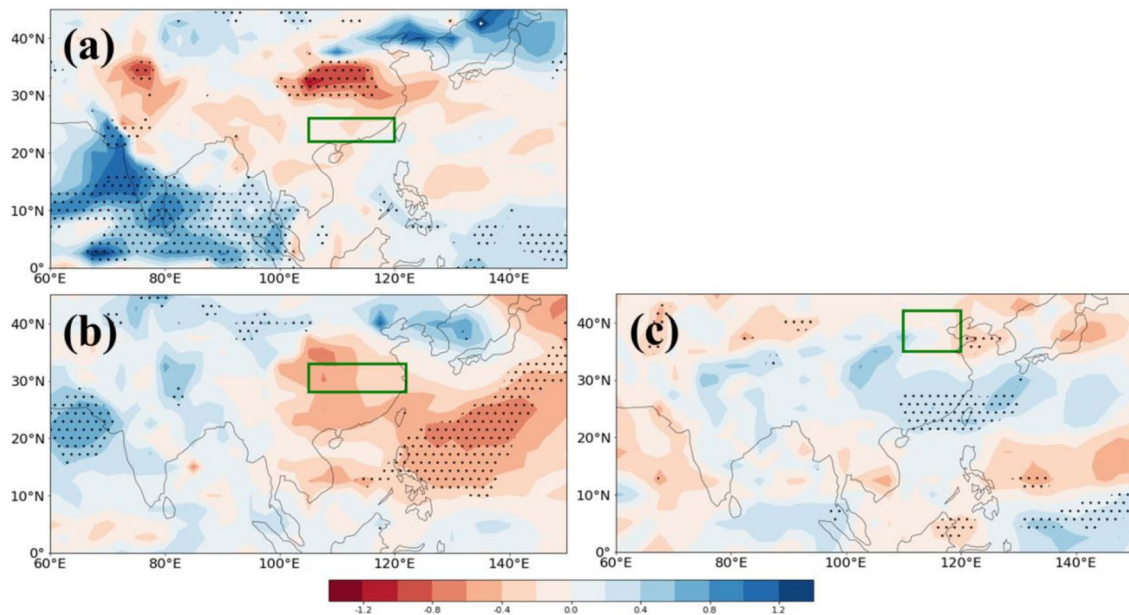
Fig. 14 Anomalies of evaporation (shade, mm) regressed on the detrend time series of **a** the IO source precipitation over SC, **b** the IO source precipitation over the YRV, and **c** the EC source precipitation over NC during PMRP (dark spotted areas denote significance at the 0.1 level)

opposite trend is observed when the zonal moisture transport is enhanced. Figure 13a shows the differences in the water vapor transport over SC during P1. The westerly moisture transport anomalies over southeastern China, the southerly moisture transport anomalies over the South China Sea, and the northerly water vapor transport anomalies over the western North Pacific manifest a clockwise gyre pattern, meaning that the climatic clockwise moisture transport over the South China Sea connected with the subtropical high is strengthened during the strong rainfall years of SC. At the same time, there is an obviously positive anomaly in the Indian-summer-monsoon-controlled water vapor transport, which primarily carries the water vapor from the IO source through the Arabian Sea-India-Bay of Bengal-Indochina Peninsula-Southwest China-SC moisture transport branch. The enhanced IO source water vapor transport leads to a significant positive anomaly in the rainfall over SC during strong precipitation years. Figure 14a shows that the IO source water vapor that arrives and releases over SC primarily originates from the Bay of Bengal, South India, and the Arabian Sea.

Figure 13b shows the differences between the P2 moisture transport of the strong and weak precipitation years of the YRV. Climatically, during P2, the edge of the anomalous anticyclone over the western North Pacific gradually moves northwestward, resulting in southerly moisture transport anomalies reaching the YRV via the western bound of the western Pacific subtropical high. During the strong rainfall years of the YRV, the zonal water vapor transport over the YRV and the meridional water vapor transport

over the South China Sea and SC are enhanced significantly (Fig. 13b). This enhanced water vapor transports were mainly influenced by the enhancement of the subtropical high and Indian summer monsoon. Hence, through the Bay of Bengal-Indochina Peninsula-Southwest China-SC-the YRV moisture transport branch, a fair amount of water vapor from the IO source arrives and releases over the YRV. The increase in the rainfall carried by the IO source that is released over the YRV is significantly influenced by evaporation over the Arabian Sea (Fig. 14b).

Figure 13c shows the differences between the P3 moisture transport of the strong and weak precipitation years of NC, which exhibit a clockwise gyre pattern of moisture transport anomalies over the western North Pacific, meaning that the climatic clockwise moisture transport over the western North Pacific connected with the subtropical high increases during the strong rainfall years in comparison to that in the weak rainfall years. Meanwhile, the zonal water vapor transport over southeastern China weakens significantly, which leads by the weakening of the Indian summer monsoon and the strengthening of the subtropical high. Accordingly, there is an obviously positive anomaly of southerly moisture transport over East China. Therefore, for strong rainfall years in NC, the strong meridional water vapor transport, which carries water vapor from the SC source, leads to an obvious increase in rainfall. SC and the southern YRV are the primary evaporation sources of rainfall over NC (Fig. 14c).

In summary, for East China, the intensity of the subtropical high and Indian summer monsoon has an important effect on Indian-summer-monsoon-controlled water

vapor transport, which is the foremost water vapor source of rainfall during PMRPs. The spatial distribution of the IO source, PO source, and EC source rainfall is significantly affected by the position of the subtropical high. Hence, the subtropical high and Indian summer monsoon influence and may even control the amount and distribution of the summer precipitation over East China. In addition, note that the anomalous anticyclone in the background circulation during summer provided unfavorable climatic conditions for PO source water vapor transport. Thus, the PO source water vapor transport hardly influences the interannual variation in the rainfall over SC and the YRV during PMRPs.

5 Conclusions and discussion

This study uses the Lagrangian method and areal source-receptor attribution method to illustrate the effects of water vapor transport on the intraseasonal and interannual variations in the summer monsoon rainfall over East China. In this paper, three key issues of the moisture sources of East China summer precipitation are discussed: the identification of the primary moisture sources of summer precipitation, determination of their individual contributions to the intraseasonal variation in summer precipitation, and determination of the extent to which each source affects the interannual variation in the precipitation during the PMRP. The main findings of this study focus on the following aspects.

Based on the water vapor branches debated by previous studies, the water vapor sources for East China are defined by six categories. The southwesterly water vapor transport, which includes the IO source and SCS source water vapor transport, is the primary source of the summer monsoon rainfall over SC and the YRV. Considering the water vapor lost en route, the amount of Indian-summer-monsoon-controlled water vapor decreases during transport. The southeasterly moisture transport mainly releases moisture over the southeastern YRV and eastern SC. The influence of the LD source moisture transport is mainly limited to NC. The amount of EC source precipitation and recycled precipitation over SC remains low, whereas there is a large amount of EC source precipitation and recycled rainfall over the YRV and NC.

The intraseasonal variations in the summer monsoon rainfall over the YRV and SC are fundamentally influenced by the Indian-summer-monsoon-controlled water vapor transport. The intraseasonal variation in the summer monsoon rainfall over NC is fundamentally influenced by both the Indian-summer-monsoon-controlled and East-Asian-summer-monsoon-controlled water vapor transport, which mainly carries the water vapor from the YRV and SC. The amount and distribution of summer precipitation during PMRPs are significantly affected by the persistent

rainfall over East China. The rainfall contribution from the primary moisture source dominates the spatiotemporal characteristics of the rainfall during PMRPs. Thus, the IO source moisture transport determines the interannual variation in the peak monsoon rainfall over the YRV and SC. The interannual variation in the summer monsoon rainfall over NC is significantly affected by the EC source moisture transport, which is mainly affected by the Indian-summer-monsoon-controlled water vapor transport.

The intensity of the subtropical high and Indian summer monsoon has an important effect on the Indian-summer-monsoon-controlled water vapor transport, which is the foremost water vapor source of rainfall during PMRPs. The spatial characteristics of the IO source and EC source rainfall are significantly affected by the position of the subtropical high. Hence, the subtropical high and Indian summer monsoon influence and may even control the spatiotemporal characteristics of summer monsoon rainfall over East China. Moreover, the PO source water vapor transport plays an important role in the interannual variation in the peak monsoon rainfall over NC.

In this study, the effects of water vapor transport on the intraseasonal and interannual variations in rainfall over East China during PMRPs are discussed. During PMRPs, oceanic moisture transport has the most important impact on the rainfall over East China. The relationships between the low-frequency modes and the precipitation originating from each moisture source should be studied further. Furthermore, although the PO source moisture transport has minimal influence on the peak monsoon rainfall over East China, the water vapor contribution from the PO source during the period after P3 greatly increases. Hence, the PO source moisture transport may need to be analyzed in future research, which will require more calculations and discussions. Note that because of the disadvantages of the Lagrangian model, only one "evaporation (uptake)-precipitation (release)" cycle is considered in the current study. The analysis of multicycle processes may be necessary for future research, which will necessitate more computations and discussions.

Moreover, the intraseasonal variations in the moisture contributions from target regional evapotranspiration sources are quite different. For NC, during the PMRP, the increase in the NC source precipitation is significantly affected by the increase in the EC source precipitation. However, for the YRV and SC, the YRV source and SC source precipitation are constant during PMRPs. Because of the southerly water vapor transport over East China during PMRPs, a fair amount of water vapor originated from the YRV source and SC source transport released over NC. This means that the EC source rainfall over NC is fundamentally affected by the evapotranspiration over the YRV and SC (Fig. 14c). Considering the delaying effect

of summer rainfall (Ma et al. 2004; Pathak et al. 2014), the evapotranspiration over the YRV and SC during P3 (P2) is significantly affected by the precipitation over the YRV and SC during P2 (P1). Therefore, the relationship between the precipitation over SC during P2 and the precipitation over NC during P3 is worth studying.

References

Brimelow CJ, Reuter WG (2005) Transport of atmospheric moisture during three extreme rainfall events over the Mackenzie River Basin. J Hydrometeorol 6(4):23–440

Chan JCL, Zhou W (2005) PDO, ENSO and the early summer monsoon rainfall over south China. Geophys Res Lett 32(8):93–114

Chen Y, Luo YL (2018) Analysis of paths and sources of moisture for the south China rainfall during the Presummer rainy season of 1979–2014. J Meteorol Res 32:744–757

Chen B, Xu XD, Shi XH (2011) Estimating the water vapor transport pathways and associated sources of water vapor for the extreme rainfall event over east of China in July 2007 using the Lagrangian method. Acta Meteorol Sin 69(05):810–818 (**In Chinese**)

Chu QC, Wang QG, Qiao SB, Feng GL (2015) Spatial-temporal characteristics of the "cumulative effect" of torrential rain over South China. Theor Appl Climatol 127:911–921

Chu QC, Wang QG, Qiao SB, Feng GL (2016) Feature analysis and primary causes of pre-flood season "Cumulative Effect" of Torrential Rain over South China. Theor Appl Climatol 131(1–2):91–100

Chu QC, Wang QG, Feng GL (2017) Determination of the major moisture sources of cumulative effect of torrential rain events during the preflood season over South China using a Lagrangian particle model. J Geophys Res 122(16):8369–8382

Chu QC, Wang QG, Feng GL (2019a) The roles of moisture transports in intraseasonal precipitation during the preflood season over South China. Int J Climatol. https://doi.org/10.1002/joc.6329

Chu QC, Zhi R, Wang QG, Feng GL (2019b) Roles of moisture sources and transport in precipitation variabilities during boreal summer over East China. Clim Dyn 53:5437–5457

Coching C (1934) The enigma of southeast monsoon in China. Acta Geogr Sin 1:1–27 (**In Chinese**)

Ding YH, Chan JCL (2005) The East Asian summer monsoon: an overview. Meteorol Atmos Phys 89:117–142

Ding YH, Wang ZY, Sun Y (2008) Inter-decadal variation of the summer precipitation in East China and its association with decreasing Asian summer monsoon. Int J Climatol 28(9):1139–1161

Ding YH, Sun Y, Wang ZY, Zhu YX, Song YF (2009) Inter-decadal variation of the summer precipitation in China and its association

with decreasing Asian summer monsoon part II: possible causes. Int J Climatol 29(13):1926–1944

Dominguez F, Kumar P, Liang X, Ting M (2006) Impact of atmospheric moisture storage on precipitation recycling. J Clim 19:1513–1530

Draxler RR, Hess GD (1997) Description of the HYSPLIT_4 Modeling System. NOAA Technical Memorandum ERL ARL, pp 197–199

Draxler RR, Hess GD (1998) An overview of the HYSPLIT_4 modeling system of trajectories, dispersion, and deposition. Aust Meteorol Mag 47(4):295–308

Drumond A, Nieto R, Gimeno L (2011) On the contribution of the Tropical Western Hemisphere Warm Pool source of moisture to the Northern Hemisphere precipitation through a Lagrangian approach. J Geophys Res Atmos 116(D21):2–3

Emil SD, Amey P, Subimal G (2016) Use of atmospheric budget to reduce uncertainty in estimated water availability over South Asia from different reanalyses. Sci Rep 6:29664

Fan K (2006) Atmospheric circulation in southern Hemisphere and summer rainfall over Yangtze River Valley. Chin J Geophys 49:599–606

Fan K, Wang HJ, Choi YJ (2008) A physically-based statistical forecast model for the middle-lower reaches of the Yangtze River Valley summer rainfall. Chin Sci Bull 53:602–609

Gimeno L, Drumond A, Nieto R, Trigo RM, Stohl A (2010) On the origin of continental precipitation. Geophys Res Lett 37:L13804

Gong ZQ, Clément H, Feng GL (2017) Methods for improving the prediction skill of summer precipitation over East Asia-West Pacific. Weather Forecast 31(4):1381–1392

Gong ZQ, Dogar M, Feng G, Let al (2019) The possible physical mechanism for the EAP-SR co-action. Clim Dyn 51(4):1499–1516

Hua L, Zhong L, Ma Z (2017) Decadal transition of moisture sources and transport in Northwestern China during summer from 1982 to 2010. J Geophys Res Atmos 122:12522–12540

Huang RH, Zhang Z, Huang G, Ren BH (1998) Characteristics of the water vapor transport in East Asian Monsoon Region and its difference from that in South Asian Monsoon Region in Summer. Acta Meteorol Sci 22(4):460–469 (**In Chinese**)

James P, Stohl A, Spichtinger N et al (2004) Climatological aspects of the extreme European rainfall of August 2002 and a trajectory method for estimating the associated evaporative source regions. Nat Hazards Earth Syst Sci 4(5–6):733–746

Jiang ZH, Ren W, Liu ZY, Yang H (2013) Analysis of water vapor transport characteristics during the Meiyu over the Yangtze–Huaihe River valley using the Lagrangian method. Acta Meteorol Sci 71(2):295–304 (**In Chinese**)

Jiang ZH, Jiang S, Shi Y, Liu Z, Li W, Li L (2017) Impact of moisture source variation on decadal scale changes of precipitation in North China from 1951 to 2010. J Geophys Res Atmos 122:600–613

Li XZ, Liang W, Wen ZP (2010) Characteristics of the atmospheric water vapor and its relationship with rainfall in South China in Northern Autumn, Winter and Spring. J Trop Meteorol 26(5):626–632 (**In Chinese**)

Li XZ, Zhou W, Li C et al (2013) Comparison of the annual cycles of moisture supply over southwest and southeast China. J Clim 26(24):10139–10158

Li XZ, Wen ZP, Chen DL, Chen ZS (2019) Decadal transition of interannual mode of moisture circulation over EA-WNP: bonding to different evolution of ENSO. J Clim 32:289–308

Ma ZG, Wei HL, Fu CB (2004) Relationship between regional soil moisture variation and climatic variability over East China. Acta Meteorol Sin 58(3):278–287 (**In Chinese**)

Pathak A, Ghosh S, Kumar P (2014) Precipitation recycling in the Indian subcontinent during summer monsoon. J Hydrometeorol 15(5):2050–2066

Pathak A, Ghosh S, Martinez JA, Dominguez F, Kumar P (2017) Role of oceanic and land moisture sources and transport in the seasonal and interannual variability of Summer Monsoon in India. J Clim 30(5):1839–1859

Perry LB, Konrad CE et al (2007) Antecedent upstream air trajectories associated with northwest flow snowfall in the southern Appalachians. Weather Forecast 22:334–351

Shen C, Wang W, Hao Z, Gong W (2007) Exceptional drought events over eastern China during the last five centuries. Clim Change 85:453–471

Si D, Xu H, Wen M, He J (2008) Analysis of the westward extension of western Pacific subtropical high during a heavy rain period over southern China in June 2005. J Trop Meteorol 14:93–96

Simmonds I, Bi D, Hope P (1999) Atmospheric water vapor flux and its association with rainfall over China in summer. J Clim 12:1353–1367

Sodemann H, Stohl A (2009) Asymmetries in the moisture origin of Antarctic precipitation. Geophys Res Lett 36(22):273–289

Stohl A, James P (2004) A Lagrangian analysis of the atmospheric branch of the global water cycle. Part I: method description, validation, and demonstration for the August 2002 flooding in central Europe. J Hydrometeorol 5:656–678

Stohl A, James P (2005) A Lagrangian analysis of the atmospheric branch of the global water cycle. Part II: moisture transports between earth's ocean basins and river catchments. J Hydrometeorol 6:961–984

Sun B, Wang HJ (2011) The recent interdecadal and interannual variation of water vapor transport over eastern China. Adv Atmos Sci 28:1039–1048

Sun B, Wang HJ (2014a) Moisture sources of semi-arid grassland in China using the Lagrangian particle model FLEXPART. J Clim 27(6):2457–2474

Sun B, Wang HJ (2014b) Analysis of the major atmospheric moisture sources affecting three sub-regions of East China. Int J Climatol 35(9):2243–2257

Sun B, Wang HJ (2015) Inter-decadal transition of the leading mode of inter-annual variability of summer rainfall in East China and its associated atmospheric water vapor transport. Clim Dyn 44:2703–2722

Trenberth KE, Fasullo JT, Mackaro J (2011) Atmospheric moisture transports from ocean to land and global energy flows in reanalyses. J Clim 24(18):4907–4924

Van der Ent RJ, Savenije Hubert HG, Schaefli B, Steele-Dunne SC (2010) Origina and fate of atmospheric moisture over continents. Water Resour Res 46:W09525

Wang HJ, Chen H (2012) Climate control for southeastern China moisture and precipitation: Indian or East Asian monsoon. J Geophys Res Atmos 117(D12):48–50

Xue F, Wang HJ, He JH (2003) Interannual variability of Mascarene high and Australian high and their influences on summer rainfall over East Asia. Chin Sci Bull 48:492–497

Zhai PM, Eskridge RE (1997) Atmospheric water vapor over China. J Clim 10:2643–2652

Zhang RH (2001) Relations of water vapor transport from Indian monsoon with that over East Asia and the summer rainfall in China. Adv Atmos Sci 18(5):1005–1017

Zhang SX, Feng GL, Zhao JH (2013) "Cumulative effect" of torrential rain in the middle and lower reaches of the Yangtze River. Acta Phys Sin 62:496 (**In Chinese**)

Zhao P, Zhang RH, Liu JP et al (2007) Onset of southwesterly wind over eastern China and associated atmospheric circulation and rainfall. Clim Dyn 28:797–811

Zhou TJ, Yu RC (2005) Atmospheric water vapor transport associated with typical anomalous summer rainfall patterns in China. J Geophys Res Atmos 110(D8):211

Zhu YL, Wang HJ, Zhou W, Ma JH (2011) Recent changes in the summer precipitation pattern in East China and the background circulation. Clim Dyn 36:1463–1473